CALT-473-6

SECOND ORDER PYRAMIDAL SLIP IN ZINC

K. H. Adams, R. C. Blish, T. Vreeland, Jr., and D. S. Wood

JANUARY 1966

*A REPORT ON RESEARCH CONDUCTED
UNDER CONTRACT FOR THE
U.S. ATOMIC ENERGY COMMISSION*

W. M. KECK LABORATORY OF
ENGINEERING MATERIALS

CALIFORNIA INSTITUTE OF TECHNOLOGY

PASADENA

CALT-473-6

California Institute of Technology
W. M. Keck Laboratory of Engineering Materials

SECOND ORDER PYRAMIDAL SLIP IN ZINC

by

K. H. Adams, R. C. Blish, T. Vreeland, Jr., and D. S. Wood

AEC Research and Development Report No. 5, under Contract No. AT(04-3)-473

January 1966

LEGAL NOTICE

This report was prepared as an account of Government sponsored work. Neither the United States, nor the Commission, nor any person acting on behalf of the Commission:

A. Makes any warranty or representation, expressed or implied, with respect to the accuracy, completeness, or usefulness of the information contained in this report, or that the use of any information, apparatus, method, or process disclosed in this report may not infringe privately owned rights; or

B. Assumes any liabilities with respect to the use of, or for damages resulting from the use of any information, apparatus, method, or process disclosed in this report.

As used in the above, "person acting on behalf of the Commission" includes any employee or contractor of the Commission, or employee of such contractor, to the extent that such employee or contractor of the Commission, or employee of such contractor prepares, disseminates, or provides access to, any information pursuant to this employment of contract with the Commission, or his employment with such contractor.

ABSTRACT

Measurements of strain, dislocation density, and dislocation velocity have been made in 99.999% Zn stressed in compression along the hexagonal axis, [0001]. Slip bands on the second order pyramid, $\langle 1\bar{2}1\bar{3}\rangle\{1\bar{2}12\}$, system were observed. The average dislocation density increases linearly with strain. The velocity of edge dislocations in slip bands obeys the relation $v = (\tau/\tau_o)^n$ with v in in./sec, $n = 8.7$, $\tau_o = 870$ lb/in.^{2}, and τ the resolved shear stress in lb/in.^{2} These observations together with measurements of the strain rate sensitivity of the flow stress show that the stress dependence of the density of moving dislocations is more important than the stress dependence of the dislocation velocity as they affect the strain rate.

I. INTRODUCTION

Plastic extension of zinc crystals in the [0001] direction was studied by Stofel and Wood [1]. Etch pit and slip line markings reported by Rosenbaum [2] indicate that zinc slips on the $\langle 1\bar{2}1\bar{3}\rangle\{1\bar{2}12\}$ slip system and such slip has been called pyramidal slip (actually second order pyramidal slip is more correct). Price [3] has reported electron microscope observations of the formation and climb of dislocation loops in the $\langle 1\bar{2}1\bar{3}\rangle\{1\bar{2}12\}$ slip system. Second order pyramidal slip may therefore be presumed to be the mode of deformation which produces plastic extension of zinc in the [0001] direction.

Compression along [0001] in zinc produces twinning, but the twinning is preceded by pyramidal slip. The critical resolved shear stress for pyramidal slip is approximately 250 psi which is considerably larger than the critical stress for basal slip in the $\langle \bar{1}2\bar{1}0\rangle(0001)$ system (approximately 20 psi). Compression tests on crystals oriented such that the load axis is [0001] produce pyramidal slip with negligible basal slip. The various crystallographic planes and directions in zinc crystals discussed in this report are illustrated in Fig. 1.

The pyramidal slip planes intersect $(10\bar{1}0)$ prism surfaces at angles of 28.3° and 47.2° to the [0001]. Dislocations intersecting surfaces near $(10\bar{1}0)$ and (0001) planes of a crystal may be revealed by the etching procedures developed by Brandt, Adams, and Vreeland [4,5]. This report presents the results of a continuing investigation of pyramidal slip in zinc. Observations on dislocation density, mobility, and the strain rate sensitivity of the flow stress are reported and compared to those in the basal slip system.

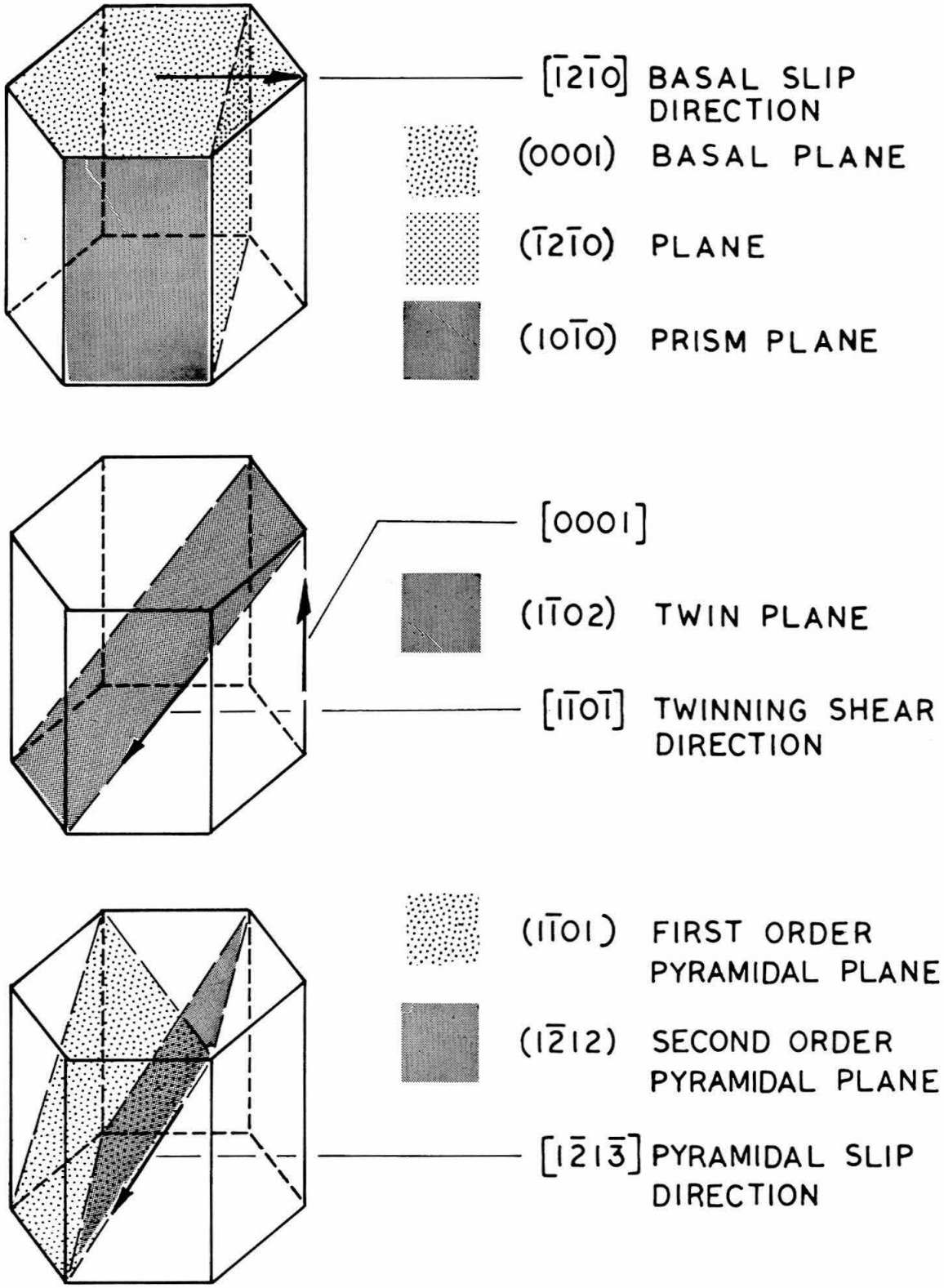

Fig. 1 Several Crystallographic Planes and Directions in Zinc Crystals.

II. MATERIAL AND SPECIMEN PREPARATION

Single crystals of zinc of 99.999% purity were prepared by the techniques described previously[6]. Specimens were machined from the crystals by the spark erosion process[6]. The dislocation mobility and strain rate sensitivity experiments employ specimens in the form of 1/2 in. cubes oriented with two (0001) surfaces to which loads are applied, two $(10\bar{1}0)$ surfaces suitable for dislocation etching, and two $(\bar{1}2\bar{1}0)$ surfaces. Cylindrical compression specimens of approximately 3/8 in. in diameter and 1 in. long with a [0001] cylindrical axis were prepared by spark erosion and finished by acid machining for stress vs. strain and strain vs. dislocation density measurements. All specimens were annealed prior to testing at 700°F in a purified hydrogen atmosphere for 4 to 8 hours.

III. TEST PROCEDURES

Static Tests

The 3/8 in. diameter compression specimens were etched and replicated to record the initial dislocation densities. The replication technique described previously was used [6]. The specimens were capped with teflon using Armstrong A-12 epoxy to fill in any surface irregularities. Two type FAP-25-12 foil strain gages obtained from the Baldwin-Lima-Hamilton Corporation were bonded to opposite sides of the specimens using SR-4 cement. Two dummy gages were mounted on another unstressed specimen. The four gages were connected in a Wheatstone bridge circuit so as to cancel bending strain in the specimen. The output of the strain gage bridge was amplified and recorded on one axis of an x-y recorder.

Tests were carried out in an Instron Universal testing machine using a cross head speed of 0.001 in./min. The compressive load applied to the specimen was recorded on the 2nd axis of the x-y recorder. Specimens were unloaded, etched, and replicated to record the dislocation density at various strain levels. The replicas were flashed with aluminum to make them optically opaque and 100X photomicrographs were taken for etch pit counts.

Variable Strain Rate Test

A variable strain rate test was conducted in the Instron machine. Strain rate changes were made during the test by suddenly changing the cross head speed from 2×10^{-3} in./min to 2×10^{-4} in./min and from

2×10^{-4} in./min to zero. The outputs of the load cell and strain gage bridges were recorded vs. time on a Consolidated Electrodynamic oscillograph. A load sensitivity of 100 lb. full scale was maintained throughout the test by successively shifting the zero point 100 lbs. by means of a decade switch which shunted resistors across one leg of the load cell bridge. A full scale strain sensitivity of 160×10^{-6} in./in. was maintained throughout the test by the use of shunting resistors in one leg of the strain gage bridge. The test was discontinued when a "c" axis strain of 8×10^{-4} in./in. was reached.

Direct Mobility Tests

Compression load pulses were applied to the 1/2 in. cube specimens using the air bearing compression test fixture in the rapid loading machine as previously described [6]. The $(10\bar{1}0)$ surfaces of the specimen were etched and plastic replicas of the surfaces made to record the initial dislocation configuration. The specimen was re-etched and replicated within 3 minutes after application of a load pulse.

IV. TEST RESULTS

Static Tests

A typical room temperature stress-strain curve is shown in Fig. 2. The curve shows relatively rapid work hardening after the elastic limit is exceeded. Typical areas of the replicas taken of strained and etched specimens are shown in Fig. 3. An area which exhibits pyramidal slip on six different slip systems is shown in Fig. 4. The etch pit density vs. compressive strain is shown in Fig. 5. The bars on the points indicate the range of densities observed over different areas on the $(10\bar{1}0)$ surfaces and the points represent the mean value of the etch pit counts made at a given strain.

Variable Strain Rate Test

The strain rate sensitivity of the flow stress for pyramidal slip was found to be considerably less than that for basal slip. Very small stress jumps accompany a sudden change in strain rate. The inverse strain-rate sensitivity is defined as

$$n' = \frac{\partial \ln \dot{\gamma}_p}{\partial \ln \tau}$$

or

$$n' \cong \frac{\ln(\dot{\gamma}_{p2}/\dot{\gamma}_{p1})}{\Delta\tau/\tau} \qquad (1)$$

where $\dot{\gamma}_{p2}$ is the plastic strain rate after the change

$\dot{\gamma}_{p1}$ is the plastic strain rate before the change

$\Delta\tau$ is the jump in resolved shear stress accompanying the change ($\Delta\tau \ll \tau$).

The data analysis gave an inverse strain rate sensitivity of 720 ± 10 for both increasing and decreasing strain rates.

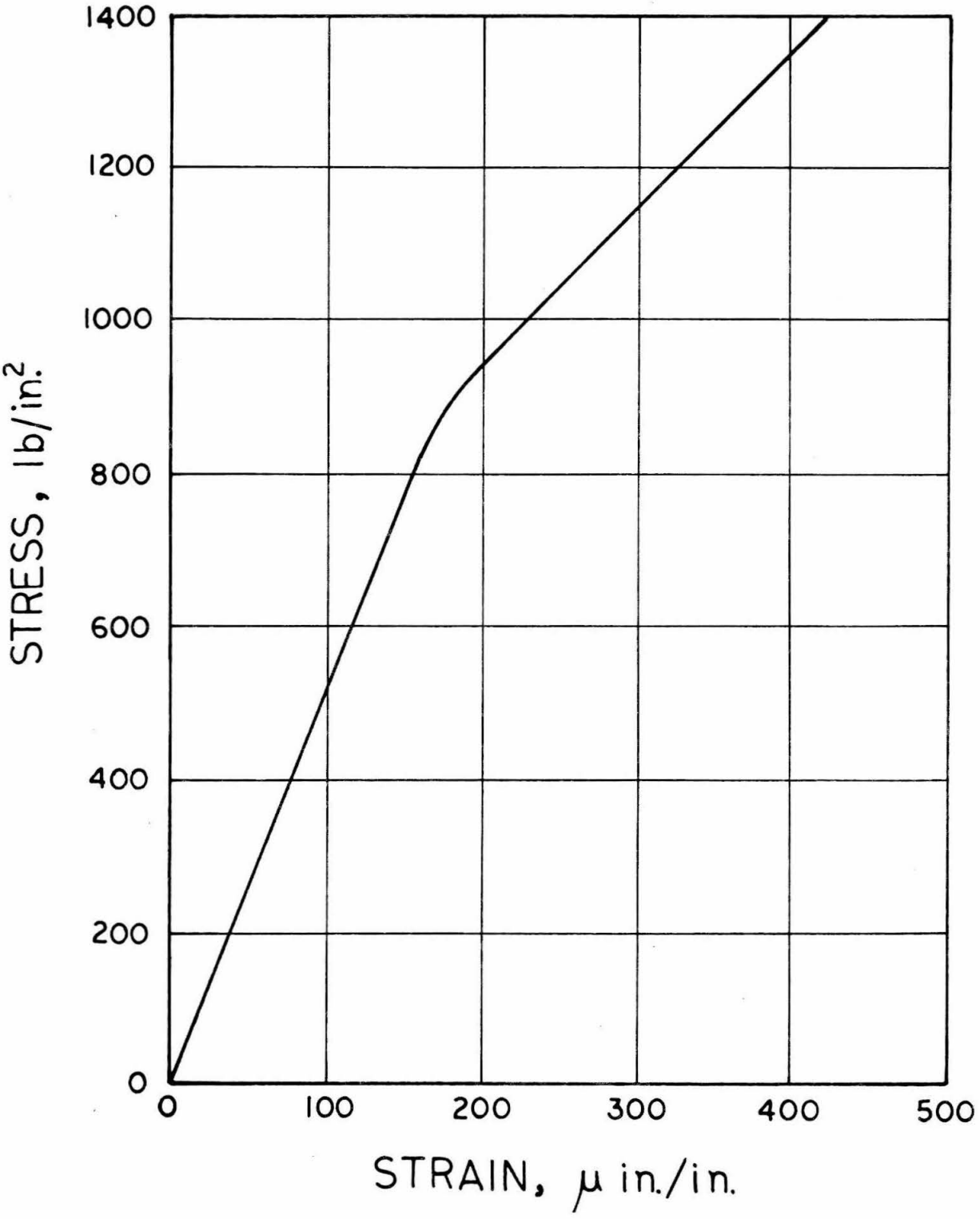

Fig. 2 Compressive Stress vs. Compressive Strain along [0001], 99.999% Zinc at Room Temperature.

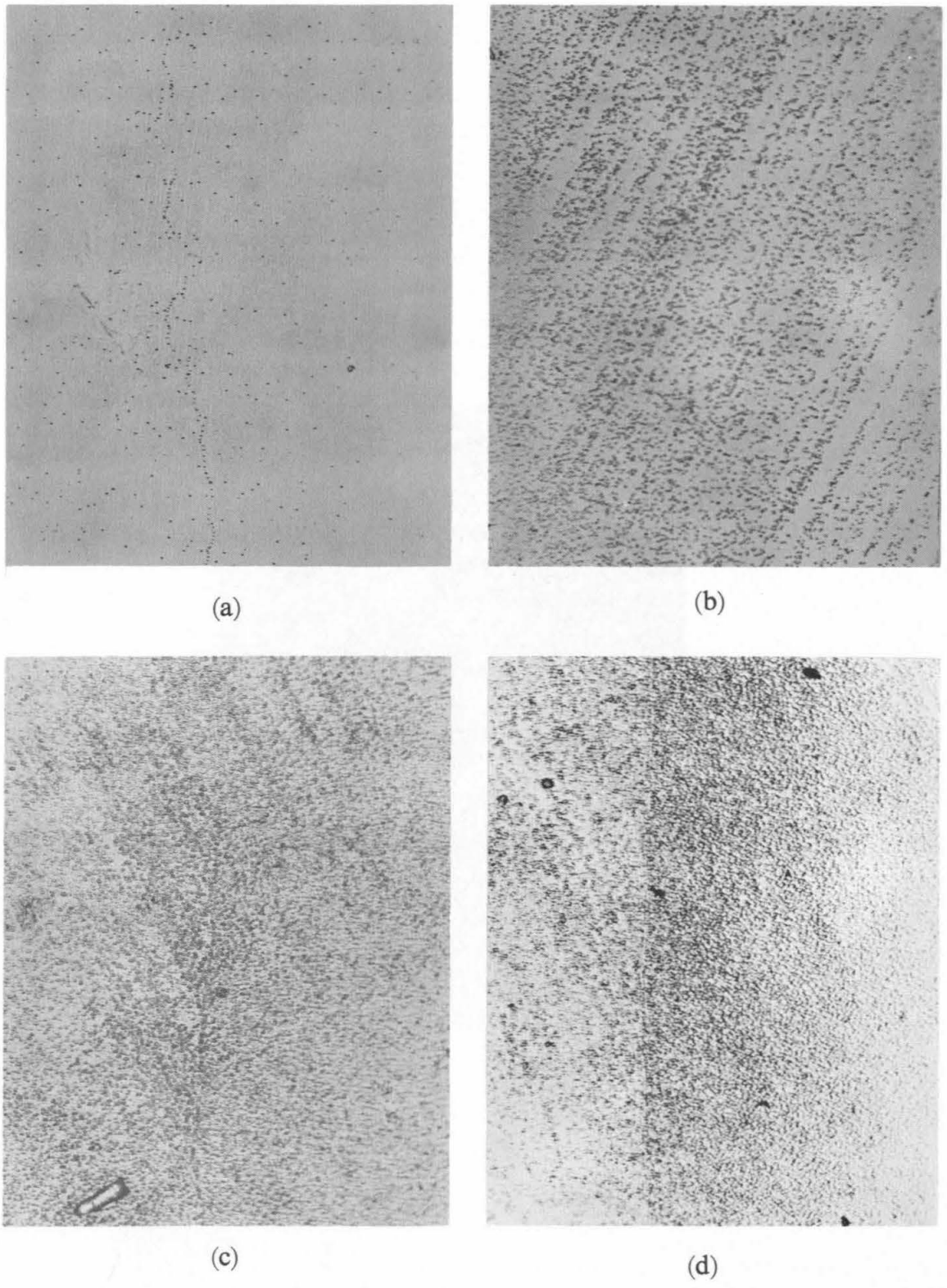

(a) (b)

(c) (d)

Fig. 3 Typical Areas of Specimens Strained in Compression along [0001], $(10\bar{1}0)$ surface, compression axis vertical, 100X. (a) no strain, (b) 132 μ in./in., (c) 270 μ in./in., (d) 395 μ in./in.

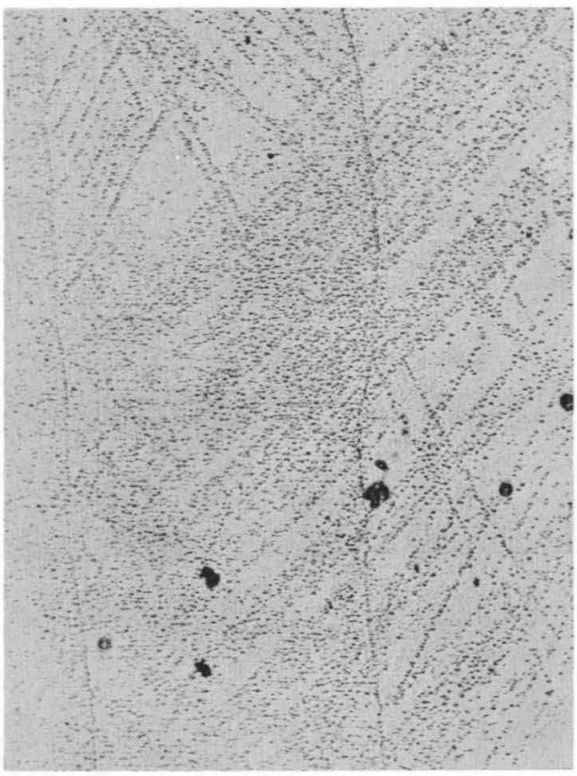

Fig. 4 An Area Showing Slip Bands on the Six Systems Intersecting the $(10\bar{1}0)$ Plane, 100X.

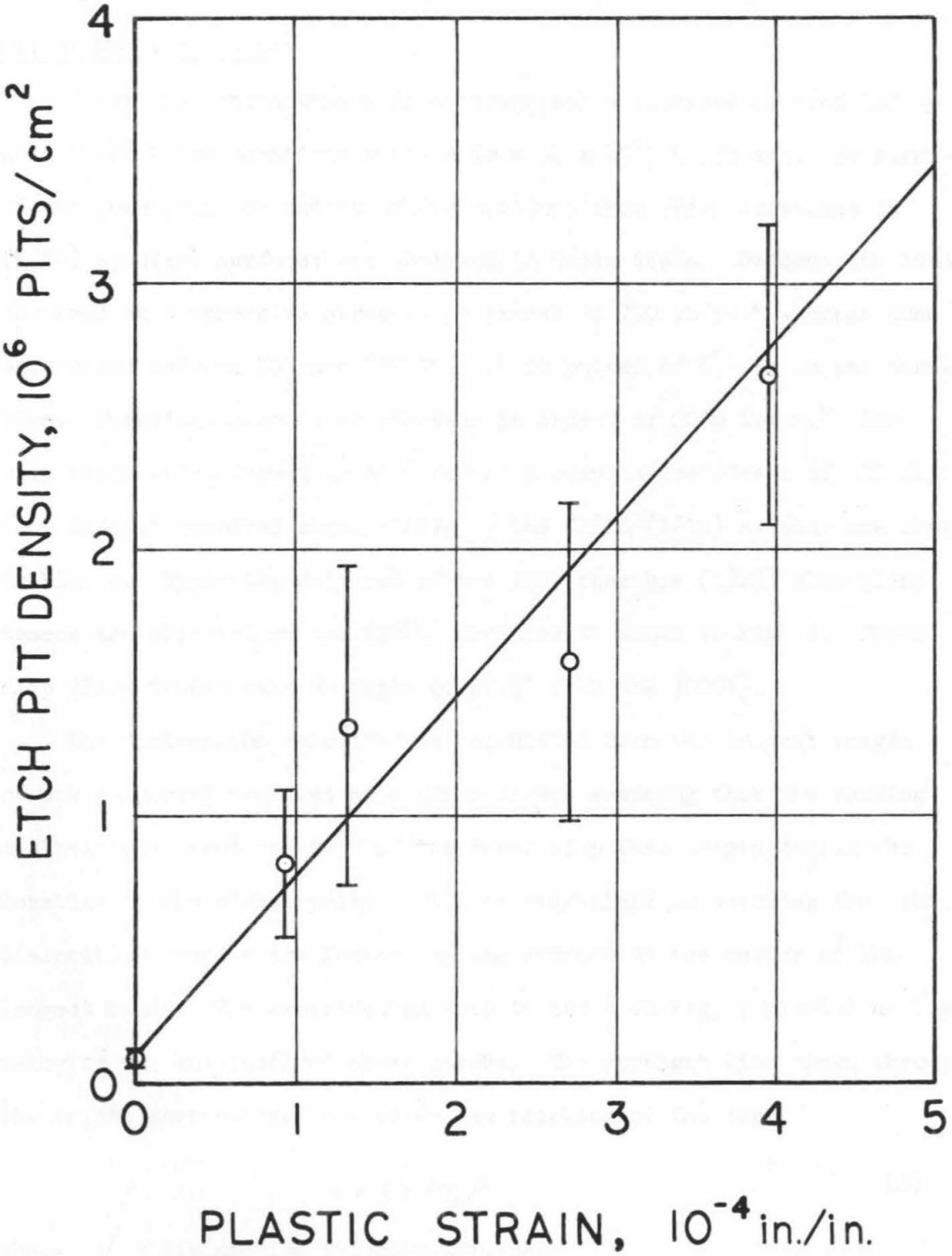

Fig. 5 Etch Pit Density on $(10\bar{1}0)$ Prism Planes vs. Compressive Strain along the [0001] Hexagonal Axis.

Direct Mobility Tests

Pulse load tests were made at compressive stresses of from 390 to 2010 lb/in.^{2} for durations ranging from 51 x 10^{-3} to 33 sec. No significant generation or motion of dislocations from fresh scratches on $(10\bar{1}0)$ specimen surfaces was observed in these tests. Deformation bands occurred at compressive stresses in excess of 790 lb/in.^{2} whereas none were found between 390 and 690 lb/in.^{2} in pulses of 6.2 to 33 sec duration. Twinning occurred at stresses in excess of 2000 lb/in.^{2} The slip bands which formed in 31.4 sec at a compressive stress of 970 lb/in.^{2} (405 lb/in.^{2} resolved shear stress in the $\langle 1\bar{2}13\rangle\{1\bar{2}12\}$ system) are shown in Fig. 6. Typically only two of the four possible $\{1\bar{2}12\}$ slip plane traces are observed on the $(10\bar{1}0)$ surfaces as shown in Fig. 6. These slip plane traces make an angle of 28.3° with the [0001].

The dislocation velocity was calculated from the longest length of new slip band produced at a given stress assuming that the leading dislocations moved one-half of the total slip band length during the duration of the stress pulse. This is equivalent to assuming that the dislocation sources are located on the surface at the center of the longest bands. The experimental data is shown in Fig. 7 plotted as log velocity vs. log resolved shear stress. The straight line drawn through the points corresponds to a power law relation of the form

$$v = (\tau/\tau_o)^n \qquad (2)$$

where v = dislocation velocity, in./sec

$n = 8.7$

τ_o = the resolved shear stress which produces a velocity of 1 in./sec and is 870 lb/in.^{2}

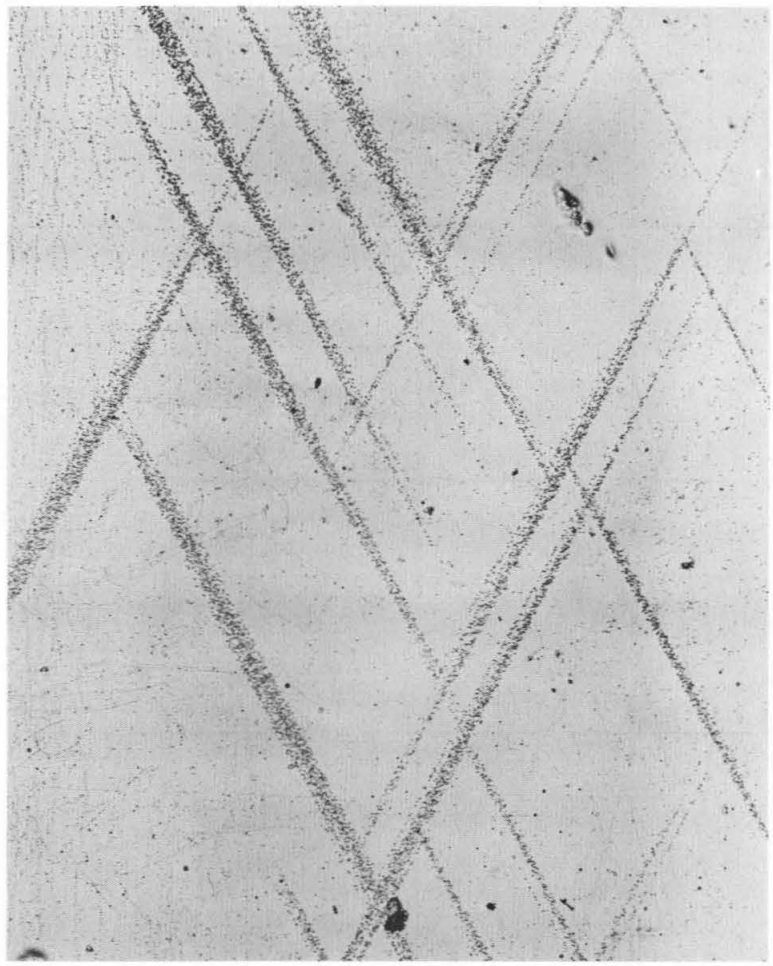

Fig. 6 Slip Bands Formed on a $(10\bar{1}0)$ Surface in 31.4 sec at a Compressive Stress of 970 lb/in.^{2}, the [0001] axis is vertical, 100X.

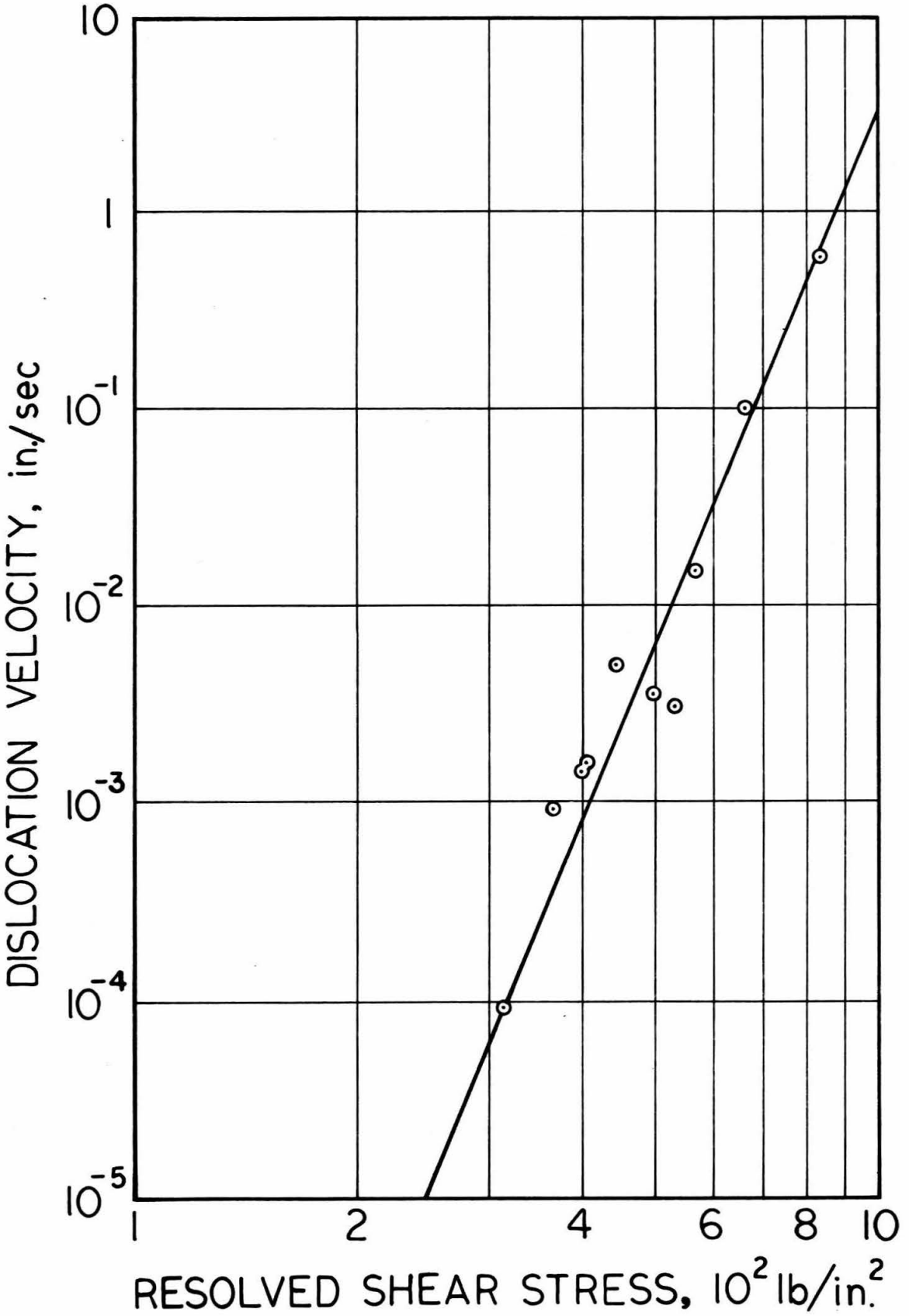

Fig. 7 Dislocation Velocity vs. Resolved Shear Stress.

A pulse loaded specimen which exhibited slip bands on $(10\bar{1}0)$ surfaces was sectioned in an attempt to observe the slip band structure in the interior of the crystal. A surface 5° from the (0001) was exposed by acid sawing the specimen essentially in half, and the surface was lapped on a cloth covered, rotating plate which was wet with a chromic acid polishing solution. The surface was then etched and compared to the adjacent $(10\bar{1}0)$ surface. Slip bands were found to extend into the crystal from the $(10\bar{1}0)$ surface considerably less than their length on that surface. The bands were not so well defined on the surface at 5° to (0001).

V. DISCUSSION

The onset of pyramidal slip on the $\langle 1\bar{2}1\bar{3}\rangle\{1\bar{2}12\}$ system is associated with the formation of slip bands. The work hardening rate in "c" axis compression is much higher than that observed in basal slip. This is in part due to the simultaneous operation of six intersecting slip systems, each equally stressed. The basal shear stress vs. shear strain curve exhibits only the stage I deformation associated with easy glide. The stress strain curve in "c" axis compression has no stage I or easy glide region. The slip bands observed on $(10\bar{1}0)$ planes cover the majority of the surface at a "c" axis strain of 10^{-4} in./in. The average density of etch pits on $(10\bar{1}0)$ surfaces increases linearly with strain up to 4×10^{-4} in./in. A considerable variation in etch pit density at a given strain is noted in different areas of the $(10\bar{1}0)$ surfaces. This is a result of the nonhomogeneous distribution of the slip bands.

The dislocation density increases with strain considerably faster in pyramidal slip than in basal slip (basal dislocation density was found to be proportional to the 1/3 power of the strain [6]). This is attributed to the relatively short slip distance of a pyramidal dislocation before cross slip takes place. Slip distances of the order of specimen dimensions were observed in basal slip with very little broadening of a slip band taking place before it extended across the specimen.

The appearance of the pyramidal slip bands on $(10\bar{1}0)$ surfaces is similar to that of slip bands in deformed single crystals of lithium fluoride [7] where dislocation multiplication has been attributed to a

multiple cross slip mechanism. Multiple cross slip occurs when a screw dislocation segment in one slip plane glides onto another slip plane which contains the same Burgers vector. Cross slip will be likely in cases where the screw dislocation is not extended into widely spaced partial dislocations and when a resolved shear stress occurs on the cross slip plane. When a screw dislocation segment glides onto the cross slip plane, it is likely to cross slip once again onto another slip plane parallel to the original slip plane. The screw segments that lie on the parallel slip plane can then act as a Frank-Read source because the dislocation segments on the cross slip plane are edge dislocations which cannot glide in the same direction as the screw segment.

Extensive cross slip was observed by Price [3] which must have occurred on $(10\bar{1}1)$ or first order pyramidal planes because this plane is the only other low index plane that contains the $[1\bar{2}1\bar{3}]$ slip direction. In addition, Price observed large dipole trails and jogs on screw dislocations and atrributed these to cross slip.

The resolved shear stress on the first order pyramidal plane is equal to about 90 per cent of that on the second order pyramidal plane in the compression tests. This produces a favorable condition for cross slip to occur and hence the conclusion is drawn that multiple cross slip is responsible for the nature of the observed slip bands.

The two slip band traces most frequently observed on the specimen prism surfaces correspond to $\{1\bar{2}12\}$ planes which make a normal intersection with the observation surface. Therefore, edge dislocations on these planes will lie perpendicular to the observation surface and screw

dislocations will lie parallel to it. The dislocations observed in the direct mobility experiment are therefore most likely close to the edge orientation with a 1/3 $\langle 1\bar{2}1\bar{3} \rangle$ Burgers vector.

The shape of a slip band appears to remain essentially constant, i.e. growth proceeds at a uniform rate in length, width, and thickness. The form of the dislocation velocity vs. stress relationship is then the same for any dislocation orientation, with the same exponent n found for edge oriented dislocations, but with increasing τ_o as the orientation goes from edge to screw.

The lower velocity for screw oriented segments is most probably a consequence of the cross slip as is the less definite shape of the slip band as viewed on a surface at 5° to the (0001). Additional tests are in progress in an attempt to measure more accurately the velocity of screw dislocations in the pyramidal slip bands.

The absence of slip bands intersecting $(10\bar{1}0)$ surfaces at 47.2° to the [0001] after pulse load tests is partially explained by the "wavy slip" nature of the growth of the slip bands in the direction of glide of the screw oriented dislocations combined with the lower velocity of screw oriented dislocations. It appears, however, that a definite preference exists for the operation of surface sources which are of edge orientation (the Burgers vector then lies in the surface). Such a preference for surface sources of a given orientation could explain the significant effect of the shape of the specimen cross section on the stress strain behavior which has been observed in single crystals.

A comparison may be made of the inverse strain rate sensitivity as determined in the strain rate test, and the mobility exponent as determined in the pulse tests. The plastic strain rate is related to the density of moving dislocations ρ_m and the average dislocation velocity v by

$$\dot{\gamma}_p = \rho_m b v \tag{3}$$

where b is the Burgers vector of the dislocations in the active slip system. The inverse strain rate sensitivity in Eq. (1) is thus

$$n' = \frac{\partial \ln \rho_m}{\partial \ln \tau} + \frac{\partial \ln v}{\partial \ln \tau} \tag{4}$$

The second term on the right hand side of Eq. (4) is the mobility exponent n of Eq. (2), which was found to be 8.7. The value of n' was determined to be 720. The difference between n' and n is considerably larger than n as found for basal dislocations in zinc [6]. The difference must be attributed to the first term on the right hand side of Eq. (4). This indicates that there is a considerable change in the density of moving dislocation with a change in stress, and the stress dependence of ρ_m is more important than the stress dependence of v as they affect the strain rate. The stress dependence of ρ_m has been neglected by some investigators, when attempting to analyze the results of variable strain rate tests [8].

VI. CONCLUSIONS

1. Zinc at room temperature deforms by slip on the $\langle 1\bar{2}1\bar{3}\rangle\{1\bar{2}12\}$ systems when subjected to compressive stresses in excess of 790 lb/in.^{2} along [0001]. The slip is observed to be initially concentrated in slip bands which cover the specimen surfaces at a strain level of approximately 10^{-4} in./in.

2. The dislocation density increases linearly with strain in the [0001] direction between 10^{-4} and 4×10^{-4} in./in.

3. The velocity of edge dislocations in slip bands follows the relation $v = (\tau/\tau_o)^n$ in./sec, with $n = 8.7$, $\tau_o = 870$ lb/in.^{2}, and τ the resolved shear stress, lb/in.^{2}

4. The stress dependence of the moving dislocation density is considerably greater than the stress dependence of the dislocation velocity in $\langle 1\bar{2}1\bar{3}\rangle\{1\bar{2}12\}$ slip.

5. A preference exists for the formation of slip bands on $(10\bar{1}0)$ surfaces on the two slip systems whose Burgers vectors lie in that surface. The two other slip systems which intersect $(10\bar{1}0)$ surfaces are seldom observed even though they are equally stressed.

REFERENCES

(1) E. J. Stofel and D. S. Wood, "Fracture of Zinc Single Crystals," Fracture of Solids. Proceedings of an International Conference, Maple Valley, Wash. August 1962, Interscience Publishers, 521.

(2) H. S. Rosenbaum, "Non-Basal Slip and Twin Accommodation in Zinc Crystals," Acta Metallurgica (1961), Vol. 9, pp. 742-748.

(3) P. B. Price, "Pyramidal Glide and the Formation and Climb of Dislocation Loops in Nearly Perfect Zinc Crystals," The Philosophical Magazine (1960), Vol. 5, Eighth Series, pp. 873-886.

(4) R. C. Brandt, K. H. Adams, and T. Vreeland, Jr., "Etching of High Purity Zinc," Journal of Applied Physics (1963), Vol. 34, pp. 587-590.

(5) R. C. Brandt, K. H. Adams, and T. Vreeland, Jr., "Dislocations and Etch Figures in High Purity Zinc," Journal of Applied Physics (1963), Vol. 34, pp. 591-594.

(6) K. H. Adams, T. Vreeland, Jr., and D. S. Wood, "Basal Dislocation Mobility in High Purity Zinc Single Crystals," CALT-473-4, AEC Research and Development Report No. 3, under Contract No. AT(04-3)-473, June 1965.

(7) W. G. Johnston and J. J. Gilman, "Dislocation Multiplication in Lithium Fluoride Crystals," Journal of Applied Physics (1960), Vol. 31, pp. 632-643.

(8) Hans Conrad, "Yielding and the Flow of the B.C.C. Metals at Low Temperatures," The Relation Between the Structure and Mechanical Properties of Metals, Vol. II, London: Her Majesty's Stationery Office.